Theor Appl Climatol (2018) 131:91–100
DOI 10.1007/s00704-016-1947-y

ORIGINAL PAPER

Feature analysis and primary causes of pre-flood season "cumulative effect" of torrential rain over South China

Qu-cheng Chu[1,2] · **Qi-guang Wang**[3] · **Shao-bo Qiao**[1] · **Guo-lin Feng**[1,2]

Received: 7 July 2016 / Accepted: 15 September 2016 / Published online: 12 October 2016

Abstract When persistent rainfall occurs frequently over South China, meso-scale and micro-scale synoptic systems persist and expand in space and time and eventually form meso-scale and long-scale weather processes. The accumulation of multiple torrential rain processes is defined as a "cumulative effect" of torrential rain (CETR) event. In this paper, daily reanalysis datasets collected by the National Centers for Environmental Prediction-Department of Energy (NCEP-DOE) during 1979–2014 are used to study the anomalous features and causes of heavy CETR events over South China. The results show that there is a significant difference in the spatial distribution of the heavy CETR events. Based on the center position of the CETR, the middle region displayed middle-region-heavy CETR events while the western region displayed west-region-heavy CETR events. El Niño events in the previous period (December, January, February, March (DJFM)) are major extra-forcing factors of middle-region-heavy CETR events, which is beneficial for the continuous, anomalous Philippine Sea anticyclone and strengthens the West Pacific Subtropical High (WPSH), extending it more westward than normal. The primary water vapor source for precipitation in middle-region-heavy CETR events is the Tropical Western Pacific Ocean. The major extra-forcing factor of a west-region-heavy CETR is the negative anomaly in the southern Tropical Indian Ocean (TIO) during the previous period (DJFM). This factor is beneficial for strengthening the cross-equatorial flow and westerly winds from the Bay of Bengal to the South China Sea (SCS) and early SCS summer monsoon onset. The primary water vapor source of precipitation in the west-region-heavy CETR is the southern TIO.

✉ Guo-lin Feng
fenggl@cma.gov.cn

[1] Physical Science and Technology College of Yangzhou University, Yangzhou 225002, China

[2] National Climate Center, CMA, Beijing 100081, China

[3] China Meteorological Administration Training Center, Beijing 100081, China

1 Introduction

Under the global warming, precipitation characteristics across the East China monsoon region have changed considerably. A significant increase in persistent torrential rain and a significant decrease in light rain have been found over East China (Zhai et al. 2005; Ding and He 2006; Bao and Huang 2006; He et al. 2015). The persistent torrential rain means that sequential torrential rains (where the daily precipitation amount exceeds 50 mm) occur at certain stations for at least 3 days (Bao 2007). Chen and Zhai (2013) analyzed the persistent torrential rain events in the central and southern parts of eastern China and found that persistent torrential rain occurred more frequently after 1990. Compared to the middle and lower reach of the Yangtze River, South China has the most precipitation and the most persistent rain processes during flood season (Li et al. 2008; Xu et al. 2009). In the pre-flood season (from July 1 to June 30, 91 days), there is a significant difference in the main cause of the precipitation before and after monsoon onset. The main type of precipitation before monsoon onset is frontal precipitation, whereas the main type after onset is monsoon precipitation (Huang and Wang 1992; Chang et al. 2000; Xu et al. 2012; Gao et al. 2013). The frontal precipitation was mainly caused by the atmospheric circulation anomaly over North Pacific Ocean, the westerly jet over North Asia and the Polar vortex; however, monsoon precipitation was mainly caused by water vapor transfer from East Asian summer monsoons and southwest summer monsoons

over the Bay of Bengal (Huang et al. 1993; Hou et al. 1998; Wang et al. 2002). Therefore, because the monsoon precipitation that leads into torrential rain occurs frequently and determining the flooding season main rain band over South China, it is unsatisfactory to study the precipitation over South China as a whole. Thus, it is necessary further classify the pre-flood season to study the precipitation over South China, especially to study the persistent torrential rain.

Over South China, persistent rainfall precipitation accounts for more than 45 % of the total precipitation in the pre-flood season (Bao and Huang 2006; Chu et al. 2015). In that place, the persistent torrential rain processes are mainly caused by the summer monsoons. When persistent rainfall occurs frequently over South China, these meso-scale and micro-scale synoptic systems will persist and expand in space and time and eventually form meso-scale and long-scale weather processes (Gao et al. 2003; Zheng et al. 2009; Feng et al. 2012a, b; Chu et al. 2015). Chu et al. (2015) focused on the accumulation of multiple torrential rain processes over South China for a period from 1960 to 2012 and defined it as the "cumulative effect" of torrential rain (CETR) process. The results show that CETR could determine the regional flooding season precipitation over South China, and even the flooding season main rain band in East China (Yu et al. 2007; Zhi et al. 2007; Zhang et al. 2013; Chu et al. 2015). Based on these CETR studies, we picked out specific CETR events to simplify the precipitation studies in the pre-flood season. Considering that the main disaster type in the pre-flood season is flooding, we chose heavy CETR years to study the characteristics and primary causes of CETR. The remainder of the article is organized as follows: Section 2 introduces the data and methods employed; in Section 3, we classify the CETR processes based on rainfall center position; Section 4 investigates atmospheric circulation anomalies and the possible source of water vapor for the pre-flood season over South China when the CETR events happened; in Section 5, the sea surface temperature (SST) anomalies of the CETR years during the previous period (December, January, February, March (DJFM)) and the corresponding period (April, May, June (AMJ)) are shown; and a summary, along with discussion, is presented in Section 6.

2 Data and methods

This paper used the China Meteorological Administration's (CMA) daily precipitation data from 740 stations over South China (16°N–26°N, 105°E–122°E) from 1979 to 2014. First, we used the data from before and after to address single missing data points by linear interpolation. We then eliminated any station for which the missing data accounted for more than 5 % of the total data (Chu et al. 2015). After the above steps, 78 stations were used in our analysis to select the CETR events (shown in Fig. 1). Daily reanalysis datasets of the NCEP/DOE with a 2.5° × 2.5° resolution from 1979 to 2014 (Kanamitsu et al. 2002) were used for the analysis of atmospheric circulation anomalies and water vapor flux anomalies when CETR events happened. Monthly SST data means were acquired from Global Sea Surface Temperature Analysis Data (COBE-SST). This data set, provided by the Japan Meteorological Agency, has a resolution of 1.0° × 1.0° and is available from 1891 to the present. The monthly SST datasets are used for the analysis of SST backgrounds in the previous and corresponding period of CETR events. To consider the respective effects of ENSO and TIO, we defined the TIO variability independent of ENSO, termed the TIO (non-ENSO). TIO (non-ENSO) is obtained by removing the ENSO-related part from the TIO SST anomaly based on a linear regression with respect to TIO (Zhou and Wu 2010; Wu et al. 2014).

In this study, we used the definition proposed by Chu et al. (2015) to select the CETR events. When the 3-day moving average of torrential rain station numbers is more than 3 and there are 8 or more days in this time span that satisfy the first condition, a CETR event is then identified. In addition, the precipitation levels of CETR were used to define the intensity of a CETR. The equation of the index (BQDI) is as follows:

$$\mathrm{BQDI}_i = \mathrm{Norm}\left(\frac{S_i}{S_m}(i = 1, 2, \ldots)\right)$$

where i is the ordinal year from 1979 to 2014, S_i is the precipitation of the pre-flood season CETR in this year, and S_m is the average precipitation of the pre-flood season CETR from 1981 to 2014. Norm(…) means the BQDI will be standardized.

In addition, empirical orthogonal function (EOF) analysis, correlation, and composite and linear regression analysis statistical methods were employed throughout the study. Statistical significance tests were computed using Student's two-tailed t test.

3 Classification of the pre-flood season CTER over South China

Figure 2 shows the BQDI and the pre-flood season precipitation excepting the CETR over South China (red line indicates the average precipitation of each year in pre-flood season). Comparing the BQDI and total precipitation series, the BQDI is highly correlated with the pre-flood season total precipitation on both inter-annual and inter-decadal scales. The correlation coefficient is 0.669 (exceeding the 99 % confidence level), whereas the correlation coefficient between the precipitation (excepting CETR) and the total precipitation is −0.047. Thus, the BQDI of the pre-flood season CETR

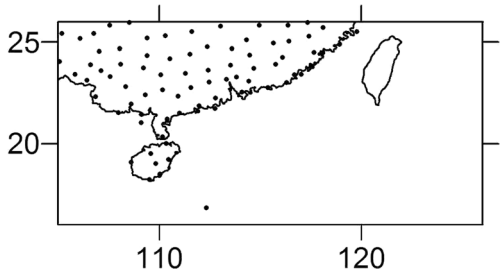

Fig. 1 Spatial distribution of 78 stations over South China

significantly determines the amount of precipitation over South China.

EOF analysis is used to analyze the frequency of torrential rain processes during the CETR periods from 1979 to 2014 (Chu et al. 2015). The results show that the cumulative first two modes account for 43 % of the total explained variance in the pre-flood season (North 1982). Figure 3 shows the spatial patterns of the first two modes and their corresponding normalized time coefficients (PC-1; PC-2). The core area of the first mode is located over central South China (shown in Fig. 3a, b). The negative phase of the first mode means that the CETR is heavy in the middle (middle-region-heavy CETR), whereas the positive phase is contrary to the negative phase. For the second mode (shown in Fig. 3c, d), the positive phase means that the CETR is heavy in the east, while light in the west (east-region-heavy CETR). In addition, the negative phase means that the CETR is heavy in the west while light in the east (west-region-heavy CETR).

To analyze the relationship between BQDI and the normalized EOF time coefficients, we sorted the BQDI in descending order and selected significantly heavy years ($BQDI \geq 0.5$). Meanwhile, we chose the years with $PC_1 \leq -1$ and $PC_1 \leq PC_2$, with $PC_2 \leq -1$ and $PC_2 < PC_1$, and with $PC_2 \geq 1$ and $PC_2 > PC_1$ as middle-region-heavy CETR, west-region-heavy CETR, and east-region-heavy CETR, respectively. The results show that the 12 significantly heavy CETR years comprised 6 middle-region-heavy CETR years, 3 west-region-heavy CETR years, and 1 east-region-heavy CETR year. In addition, all of the middle-region-heavy CETRs and west-region-heavy CETRs correspond to a heavy CETR ($BQDI > 0$). Thus, middle-region-heavy CETR and west-region-heavy CETR (shown in Table 1) were the primary types of the heavy CETR.

4 Atmospheric circulation of the pre-flood season CETR over South China

To analyze the relationship between CETR and atmospheric circulation, Fig. 4 shows the horizontal distribution of atmospheric circulation anomalies for middle-region-heavy CETR events and west-region-heavy CETR events. For middle-region-heavy CETR events, the 500-hPa geopotential height anomalies show that there are two significant positive anomalies over the tropical Pacific Ocean and the Bay of Bengal. The WPSH extends southwestward and maintains the anomalous Philippine Sea anticyclone. Meanwhile, the sea level pressure anomalies show that there is a significant negative anomaly over South China. These anomalous circulation patterns aid the strength of the southerly wind to the west of the anomalous Philippine Sea anticyclone (shown in Fig. 4a, c). Relative to its normal climatic position, the WPSH is weak and eastward when west-region-heavy CETRs occur. For west-region-heavy CETR events, there are significant negative anomalies over the Pacific Ocean and the East Indian Ocean at the 500-hPa geopotential height. The center of this anomaly is over Indochina and South China. There is also a significant positive anomaly in the sea level pressure over the southern TIO. These anomalous circulation patterns lead to a

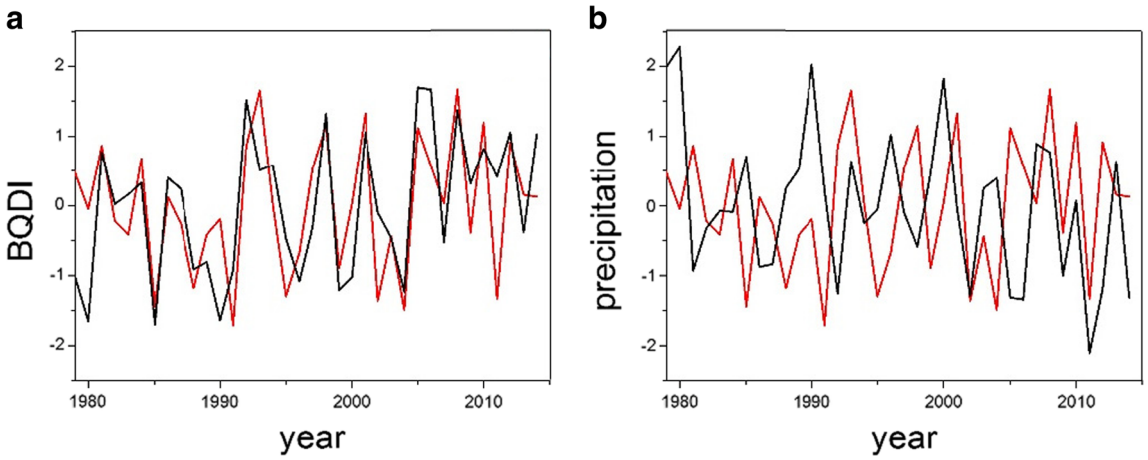

Fig. 2 Time series of the pre-flood season precipitation over South China for the period of 1979–2014: **a** BQDI and **b** the pre-flood season precipitation except the CETR (*red line* indicates the total precipitation)

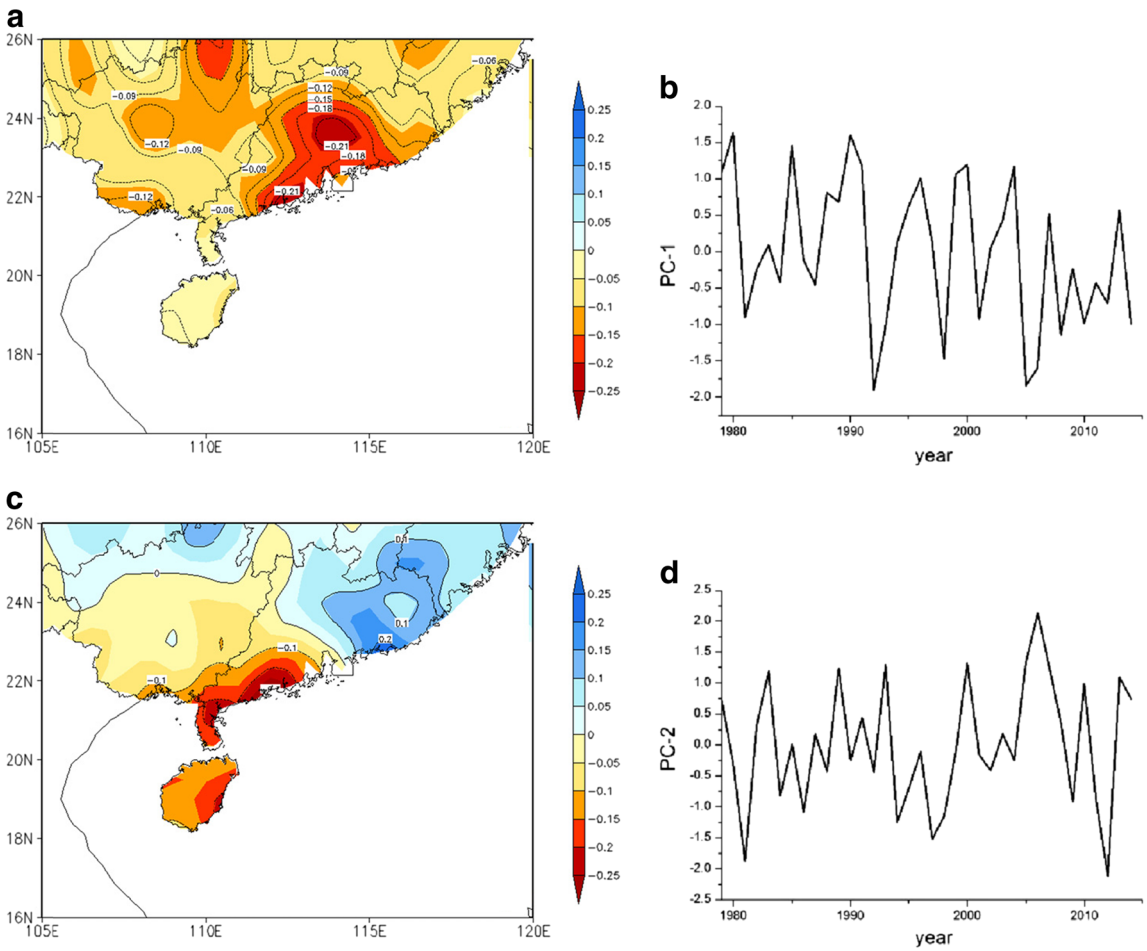

Fig. 3 The two leading EOF modes of the pre-flood season CETR over South China: **a** spatial pattern, **b** the corresponding normalized time coefficient of the first EOF mode, and **c**, **d** as in **a**, **b** but for the second mode

strengthening of the cross-equatorial flow and the positive anomaly of westerly wind from the Bay of Bengal to the SCS (shown in Fig. 4b, d).

Over South China, the pre-flood season precipitation is closely linked to the water vapor transport from other regions (Koster et al. 2004; Zhou and Yu 2005; Li et al. 2013). The vertically integrated water vapor flux anomalies associated with middle-region-heavy CETR are shown in Fig. 5a. The tropical and subtropical water vapor converged over South China. The anomalous northeastward water vapor over South China is from the SCS, but it originates from the tropical West Pacific Ocean (120°E–160°E, 5°N–10°N). The southwestward extension of the WPSH, together with the anomalous Philippine Sea anticyclone, favors the supply of the water vapor from the tropical West Pacific Ocean (Fig. 5a). The vertically integrated water vapor flux anomalies associated with west-region-heavy CETR are shown in Fig. 5b. The tropical and subtropical water vapor converged over South China and southern Indochina. There is a significant water vapor source over the southern TIO (60°E–90°E, 5°S–15°S). The water vapor from the Bay of Bengal and the cross-equator water vapor transport from the Southern Hemisphere supply the anomalous convergence over South China.

Table 1 Middle-region-heavy CETR years and west-region-heavy CETR years for the period 1979–2014

Type	Years
Middle-region-heavy CETR	1992, 1993, 1998, 2005, 2010, 2014
West-region-heavy CETR	1981, 1984, 1986, 1994, 1997, 2009, 2011, 2012

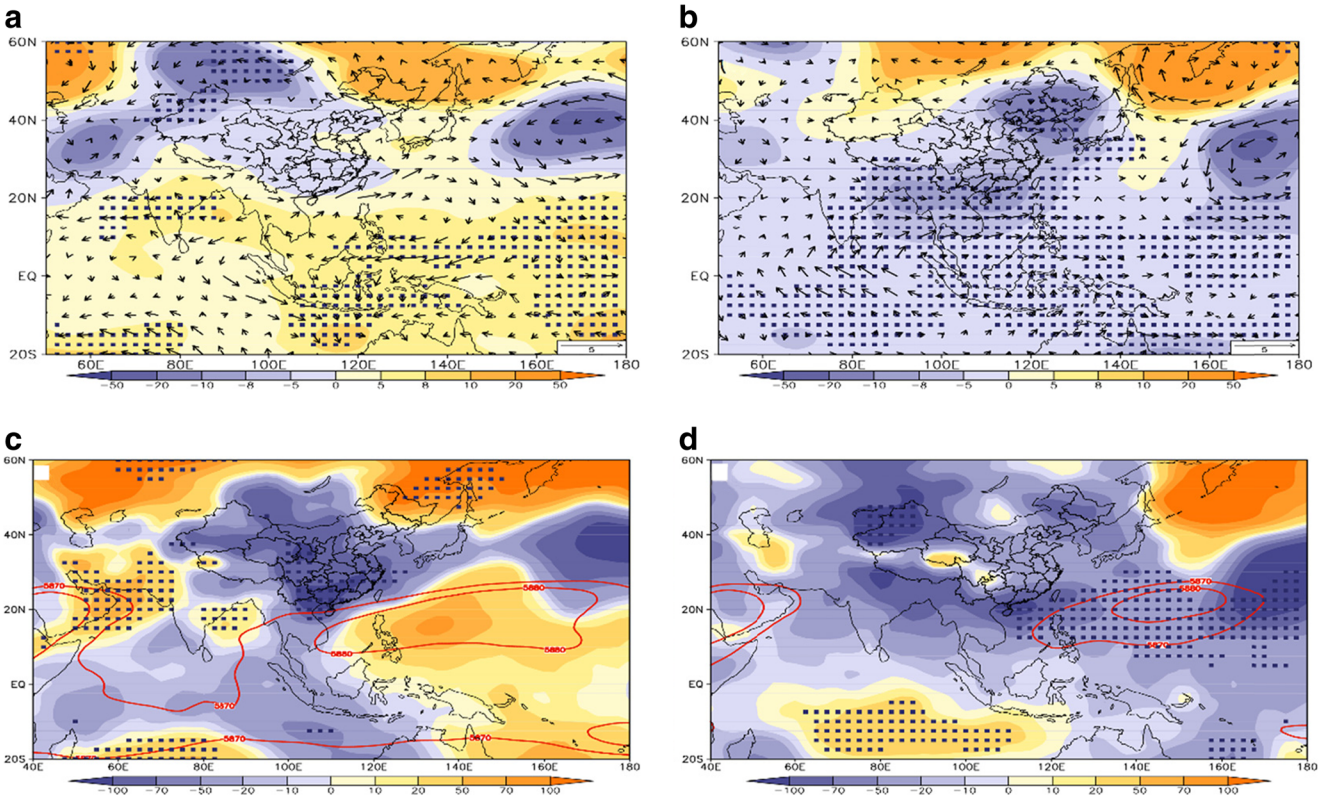

Fig. 4 The horizontal distribution of atmospheric circulation anomalies for middle-region-heavy CETR: **a** 500-hPa geopotential height (gpm) and 850-hPa wind (*arrow*, m/s), **c** sea level pressure (hPa) and WPSH (contour, 5870 gpm and 5880 gpm over 500 hPa geopotential height), and **b**, **d** as in **a**, **c** but for west-region-heavy CETR (the *dark spotted areas* show significance at the 0.05 level)

5 The pre-flood season CETR over South China associated with the SST anomalies

5.1 Middle-region-heavy CETR associated with the SST anomalies

The SST anomaly is one of the major extra-forcing drivers of atmospheric circulation (Feng et al. 2012a, b; Zhou et al. 2014). As a slow variable, the SST treated as an important subject on the seasonal scale in atmospheric science and attracts the attention of scholars worldwide (Ashok et al. 2001; Chowdary et al. 2014). The tropical West Pacific Ocean is the major water vapor source of middle-region-heavy CETR. The SST anomalies in the previous period (DJFM) and the corresponding period (AMJ) are shown in Fig. 6a, b (the dark spotted areas show significance at the 0.05 level). In DJFM, there is a significant SST warming in the El Niño region. In AMJ, the El Niño event is maintained and there is a lagging

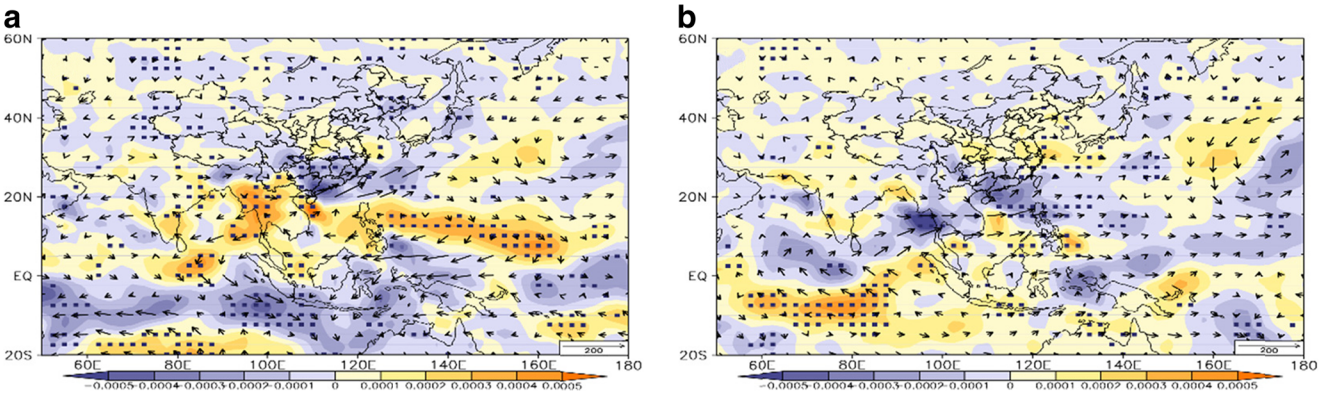

Fig. 5 The characteristics of the atmospheric water vapor transport for middle-region-heavy CETR: **a** the vertically integrated water vapor flux (*arrow*, kg/m*s) and the vertically integrated water vapor flux divergence (kg/m^2*s); **b** as in **a** but for west-region-heavy CETR (the *dark spotted areas* show significance at the 0.05 level)

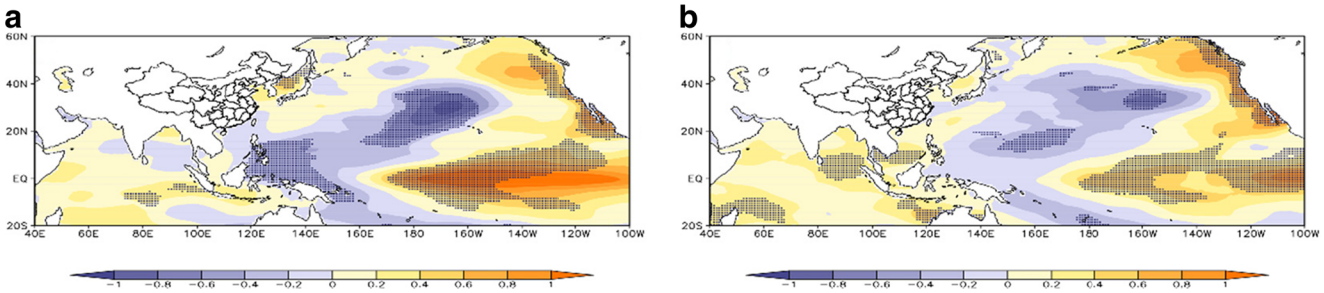

Fig. 6 The horizontal distribution of SST for middle-region-heavy CETR years: **a** DJFM and **b** AMJ (the *dark spotted areas* are significant at a 0.05 level, °C)

response of El Niño in the Bay of Bengal and SCS (Tourre and White 1995; Chambers et al. 1999; Venzke et al. 2000). These anomalies benefit the strength of the South Asia high (SAH) and the WPSH. The SAH is an eastward extension, and the WPSH is a westward extension. Under the influence of the aforementioned SST anomalies, the anomalous Philippine Sea anticyclone developed in the Indian Ocean earlier in the previous fall and was maintained over the West Pacific Ocean until the pre-flood season. The eastward passage of the anomalous Philippine Sea anticyclone appears to result from horizontal asymmetry in the moisture and temperature anomalies as well as from the existence of a large-scale divergent center over the maritime continent (Chou 2004; Chen et al. 2007). Finally, the anomalous Philippine Sea anticyclone leads to the middle-region-heavy CETR.

Table 2 shows the 3-month moving average Niño3.4 indexes in the middle-region-heavy CETR years, and Fig. 7a–f shows the SST anomalies in 6 middle-region-heavy CETR years. In the previous period, all of the middle-region-heavy CETR years have a strong SST warming in the El Niño region, except for 2014. These El Niño events last for a long time—until the pre-flood season. The SST anomalies in 2014 are similar to the SST anomalies in west-region-heavy CETR years. According to the water vapor transport anomalies in 2014, the primary water vapor transports of west-region-heavy CETR are the cross-equatorial flow, and westerly winds from the Bay of Bengal to the SCS (figure not shown). However, the strengthening of zonal westerlies leads to a middle-region-heavy CETR. In conclusion, the El Niño events in the previous period are the major extra-forcing factors of west-region-heavy CETR.

Table 2 Niño3.4 indexes in the middle-region-heavy CETR years

Years	DJF	JFM	FMA	MAM	AMJ
1992	1.6	1.5	1.4	1.2	1.0
1993	0.2	0.3	0.5	0.7	0.8
1998	2.1	1.8	1.4	1.0	0.5
2005	0.6	0.6	0.5	0.5	0.4
2010	1.3	1.1	0.8	0.5	0
2014	−0.5	−0.6	−0.4	−0.2	0
Average	0.88	0.78	0.7	0.62	0.45

5.2 West-region-heavy CETR associated with the SST anomalies

Figure 8a, b shows the SST anomalies of west-region-heavy CETR years in DJFM and AMJ. In DJFM, there are significant negative anomalies in the South TIO and tropical East Pacific Ocean. In AMJ, the La Niña event attenuated and there are significant negative anomalies in the Bay of Bengal and the SCS. Meanwhile, the negative anomalies in the Indian Ocean benefit the strength of the cross-equatorial flow and the westerly wind over the Bay of Bengal. In addition, basin-wide cooling in the TIO apparently induces an anomalous intensified Walker circulation over the tropical Indo-Pacific Ocean region, leading to anomalous ascending motion and to increased convection over the West Pacific Ocean (Yuan et al. 2008). The weakened West Pacific Ocean anticyclone in April and May favors the extension of the Indian Ocean westerly flow into the SCS region, thereby causing an early SCS summer monsoon onset. Then, west-region-heavy CETRs appear to result from the cross-equatorial water vapor transport.

To confirm the major extra-forcing factor of the west-region-heavy CETR, Fig. 9a, b shows the regression maps for AMJ's SST and 850-hPa winds for the average time series of the South TIO (0°S–10°S; 50°E–100°E) SST in DJFM before and after removing the ENSO-related portion. The negative anomaly in the southern TIO (DJFM) increases an anomalous SST (AMJ) in the SCS, the Bay of Bengal and the Northwest Pacific Ocean, strengthening the cross-equatorial flow and westerly winds from the Bay of Bengal to the SCS, leading to an anomalous cyclone over South China. Therefore, the water vapor transport from the TIO and SCS is increased. After removing the ENSO-related

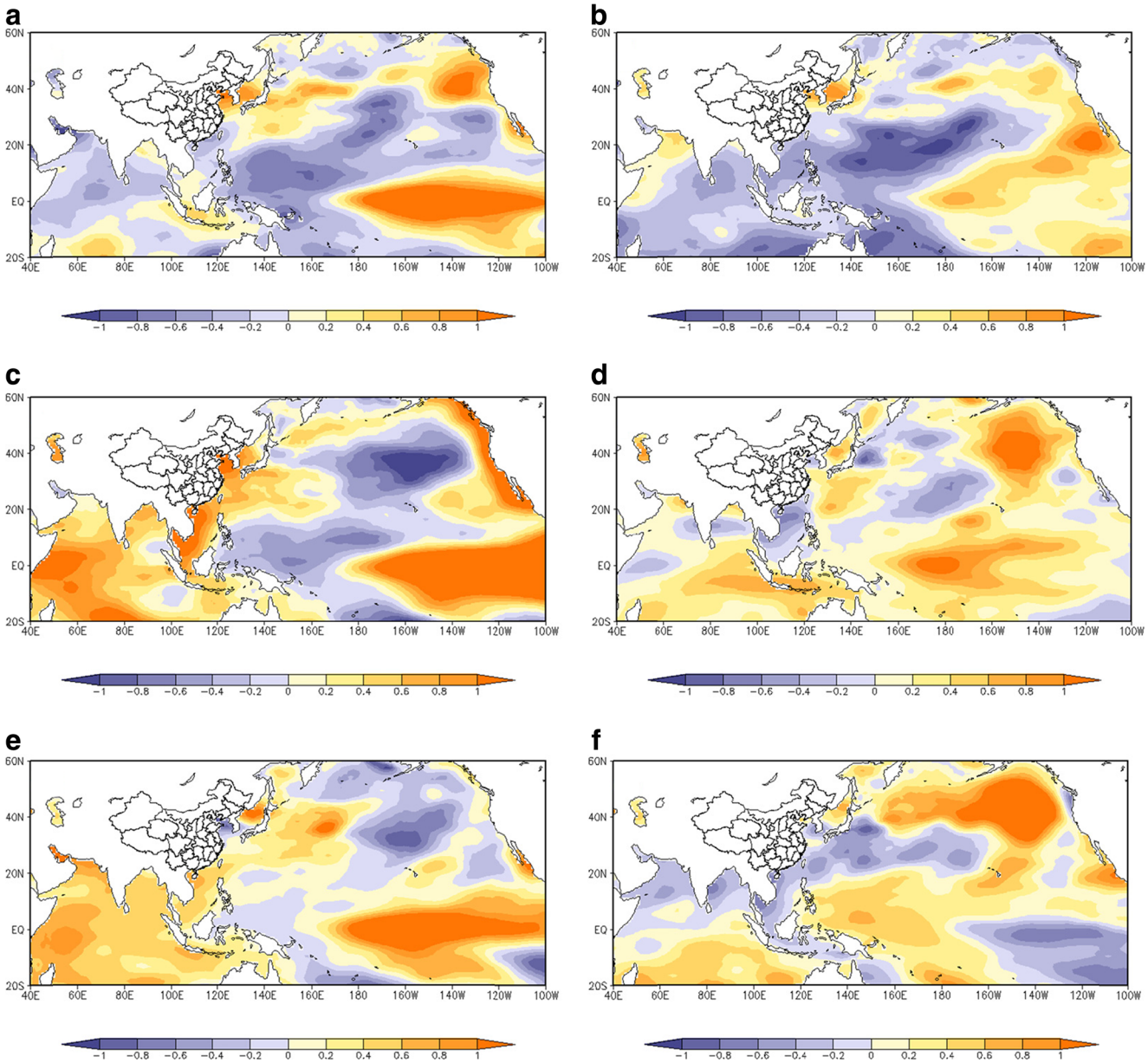

Fig. 7 The horizontal distribution of SST in DJFM: **a** 1992, **b** 1993, **c** 1998, **d** 2005, **e** 2010, and **f** 2014 (°C)

portion, anomalous SST (AMJ) in the SCS, the Bay of Bengal and the Northwest Pacific Ocean are associated with the negative anomaly in the southern TIO (DJFM). The cross-equatorial flow and westerly wind from the Bay of Bengal

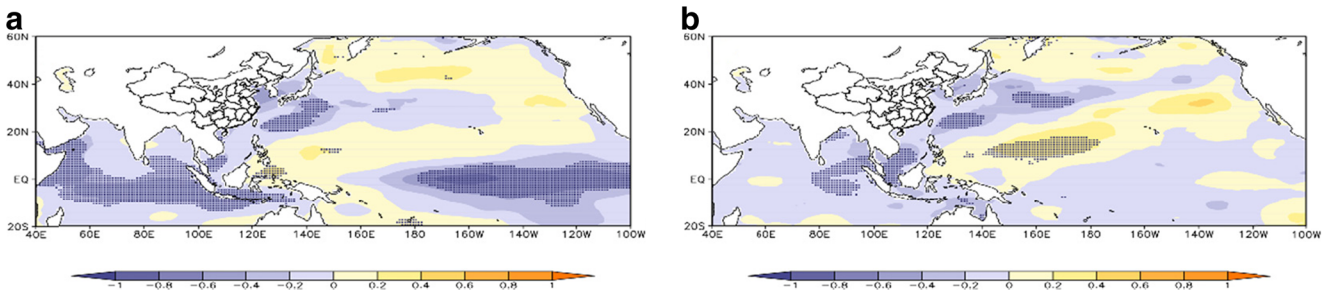

Fig. 8 The horizontal distribution of SST for west-region-heavy CETR years: **a** DJFM and **b** AMJ (the *dark spotted areas* are significant at a 0.05 level, °C)

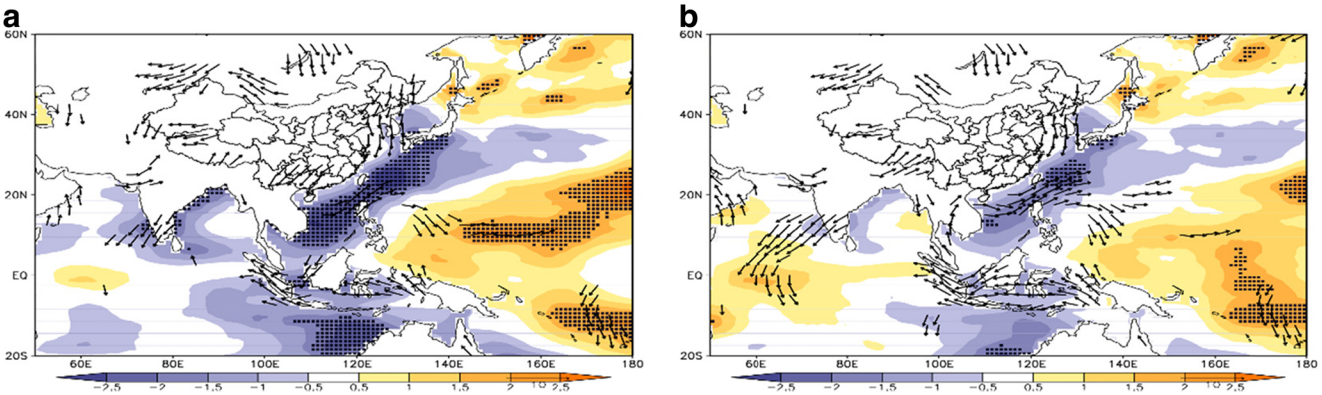

Fig. 9 **a** Regression maps for AMJ's SST and 850-hPa wind on the average time series of the southern TIO SST in DJFM. **b** as in **a** but with the ENSO-related portion removed (the *dark spotted areas* and *arrows* show significance at the 0.05 level)

to the SCS are also associated with the negative anomaly in the southern TIO (DJFM).

Furthermore, Table 3 shows the 3-month moving average Niño3.4 indexes in the west-region-heavy CETR years and Fig. 10a–h shows the SST anomalies in 8 west-region-heavy CETR years. In the previous period, all of the west-region-heavy CETR years have a negative anomaly in the southern TIO, and 7 years are accompanied by a weak La Niña event. However, all of the La Niña events had declined before the pre-flood season. Therefore, the major extra-forcing factor of the west-region-heavy CETR is the negative anomaly in the southern TIO during the previous period.

6 Discussion and conclusion

In this paper, we analyzed the distribution of CETR events over South China instead of the whole precipitation distribution over South China. Then, the primary causes of pre-flood season CETR were studied. From the present study, we draw the following conclusions:

Table 3 Niño3.4 indexes in the west-region-heavy CETR years

Years	DJF	JFM	FMA	MAM	AMJ
1981	−0.2	−0.4	−0.4	−0.3	−0.2
1984	−0.5	−0.3	−0.3	−0.4	−0.4
1986	−0.4	−0.4	−0.3	−0.2	−0.1
1994	0.1	0.1	0.2	0.3	0.4
1997	−0.5	−0.4	−0.2	0.1	0.6
2009	−0.8	−0.7	−0.4	−0.1	0.2
2011	−1.3	−1.1	−0.8	−0.6	−0.3
2012	−0.7	−0.6	−0.5	−0.4	−0.3
Average	−0.54	−0.48	−0.34	−0.2	−0.01

Analysis of the relationship between the BQDI and the normalized EOF time coefficients showed a significant difference in the spatial distribution of the heavy CETR. Based on the rainfall center position, the distributions of CETR were classified. The results show that middle-region-heavy CETR and west-region-heavy CETR were the primary types of the heavy CETR.

The atmospheric circulation and vertically integrated water vapor flux associated with pre-flood season CETR were studied. For middle-region-heavy CETR, the WPSH extends southwestward and the anomalous Philippine Sea anticyclone maintained until the pre-flood season. The anomalous northeastward subtropical water vapor over South China comes from the SCS but has a tropical West Pacific Ocean (120°E–160°E, 5°N–10°N) origin. Relative to its normal climatic position, there is a strengthening of cross-equatorial flow and a positive anomaly of westerly winds from the Bay of Bengal to the SCS when the west-region-heavy CETR occurred. There is also a significant water vapor source over the southern TIO (60°E–90°E, 5°S–15°S).

In the analysis of the SST anomalies for the previous (DJFM) and corresponding (AMJ) periods, the results show that El Niño events in the previous period are the major extra-forcing factor of middle-region-heavy CETRs; this anomaly is beneficial for strengthening the WPSH and maintaining the anomalous Philippine Sea anticyclone. The major extra-forcing factor of west-region-heavy CETRs is the negative anomaly in the southern TIO during the previous period; this anomaly is beneficial for strengthening the cross-equatorial flow and westerly wind from the Bay of Bengal to the SCS.

Remarkably, both El Niño events and the negative anomaly in the southern TIO corresponded to a heavy pre-flood season CETR over South China. Both the Pacific Ocean SST and the Indian Ocean SST are the major extra-forcing factors of heavy pre-flood season CETR over South China. However, different major extra-forcing factors lead to different water vapor transport and produce different distributions. Through the use of

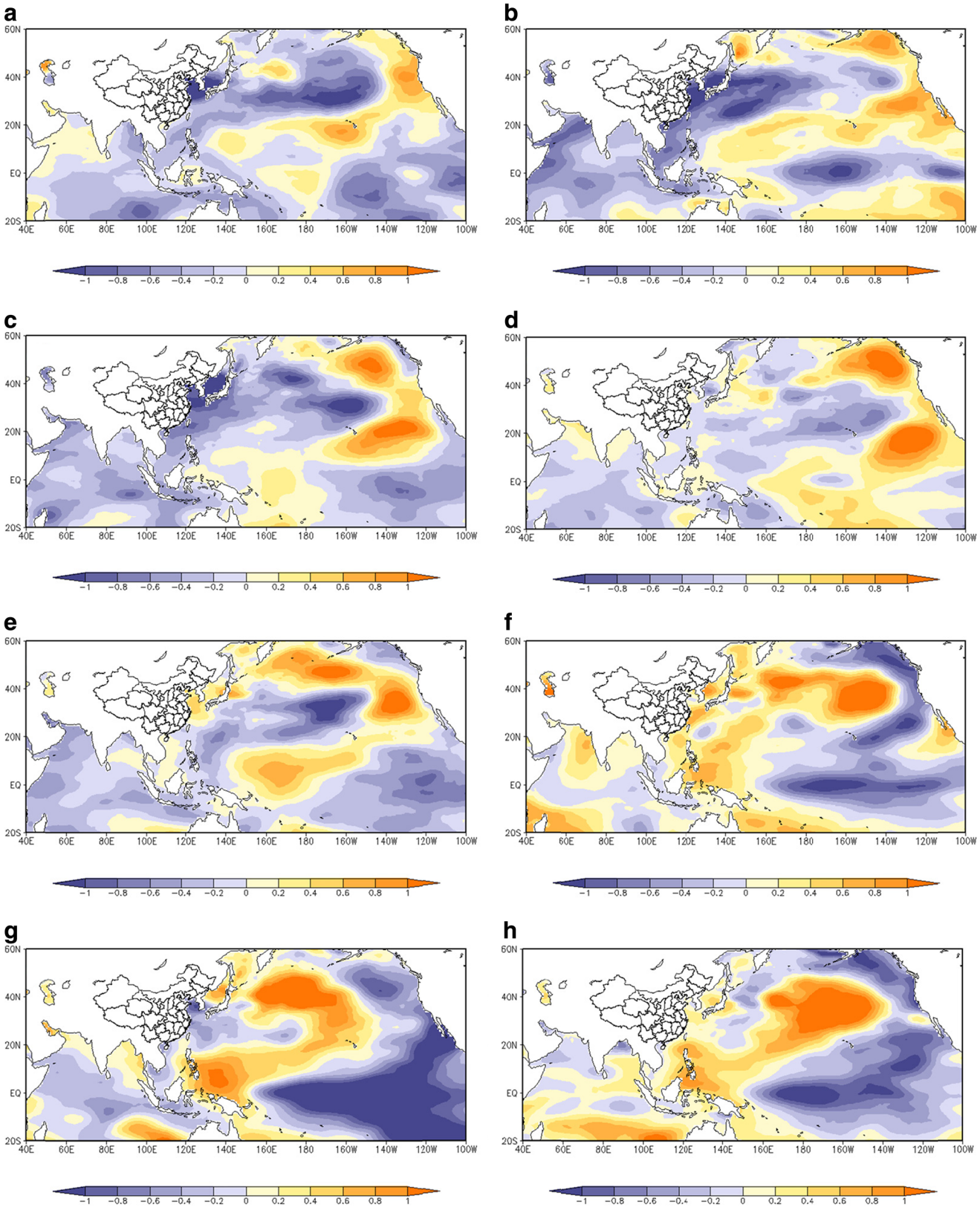

Fig. 10 The horizontal distribution of SST in DJFM: **a** 1981, **b** 1984, **c** 1986, **d** 1994, **e** 1997, **f** 2009, **g** 2011, and **h** 2012 (°C)

CETR, we can analyze the distribution of CETR events over South China instead of the whole precipitation distribution. CETR is also beneficial for studying the primary causes and the pivotal water vapor sources of the pre-flood season over

South China in meso- and long-term scales. In addition, the periods of CETR in the pre-flood season can be studied through a combination of the Madden-Julian Oscillation. Based on this study, these problems merit further careful research.

Acknowledgments This research was jointly supported by The National Natural Science Foundation of China (Grant Nos. 41375078, 41530531, 41305059, 41305100) and the National Science and Technology Support program under Grant No. 2015BAC03B06.

References

Ashok K, Guan Z, Yamagata T (2001) Impact of the Indian Ocean dipole on the relationship between the Indian monsoon rainfall and ENSO. Geophys Res Lett 28(23):4499

Bao M (2007) The statistical analysis of the persistent heavy rain in the last 50 years over China and their backgrounds on the large scale circulation. Chin J Atmos Sci 31(5):779 (in Chinese)

Bao M, Huang RH (2006) Characteristics of the interdecadal variations of heavy rain over China in the last 40 years. Chin J Atmos Sci 30:1057 (in Chinese)

Chambers DP, Tapley BD, Stewart RH (1999) Anomalous warming in the Indian Ocean coincident with El Niño. J Geophys Res 104(C2):3035

Chang CP, Zhang Y, Li T (2000) Interannual and interdecadal variations of the east Asian summer monsoon and tropical pacific SSTs. Part II: meridional structure of the monsoon. J Clim 13(24):4326

Chen Y, Zhai PM (2013) Persistent extreme precipitation events in China during 1951-2010. Clim Res 57(2):143

Chen JM, Li T, Shih CF (2007) Fall persistence barrier of sea surface temperature in the South China Sea associated with ENSO. J Clim 20(2):158

Chou C (2004) Establishment of the low-level wind anomalies over the western North Pacific during ENSO development. J Clim 17(11): 2195

Chowdary JS, Chaudhari HS, Gnanaseelan C et al (2014) Summer monsoon circulation and precipitation over the tropical Indian Ocean during ENSO in the NCEP climate forecast system. Clim Dyn 42(7–8):1925

Chu Q, Wang Q, Qiao S et al (2015) Spatial-temporal characteristics of the "cumulative effect" of torrential rain over South China. Theor Appl Climatol. doi:10.1007/s00704-015-1669-6

Ding YH, He C (2006) The summer monsoon onset over the tropical eastern Indian Ocean: the earliest onset process of the Asian summer monsoon. Adv Atmos Sci 23(6):940

Feng GL, Yang HW, Zhang SX (2012a) A preliminary research on the reason of a sharp turn from drought to flood in the middle and lower reaches of the Yangtze River in late spring and early summer of 2011. Chin J Atmos Sci 36(5):1009 (in Chinese)

Feng A, Gong Z, Wang Q et al (2012b) Three-dimensional air–sea interactions investigated with bilayer networks. Theor Appl Climatol 109(3–4):635

Gao ST, Zhao SX, Zhou XP, Sun SQ, Tao SY (2003) Progress of research on sub-synoptic scale and mesoscale torrential rain systems. Chin J Atmos Sci 27:618 (in Chinese)

Gao H, Wei J, Li W (2013) Transition of the annual cycle of precipitation from double-peak mode to single-peak mode in South China. Chin Sci Bull 58(32):3994

He W, Zhao S, Liu Q et al (2015) Long-range correlation in the drought and flood index from 1470 to 2000 in eastern China. Int J Climatol 36:1676

Hou SC, Kuo HC, Chen GT (1998) The development of an intense East Asian summer monsoon disturbance with strong vertical coupling. Mon Weather Rev 126(10):2692

Huang J, Wang S (1992) The experiment of seasonal prediction using the analogy-dynamical mode. Sci China B 35(2):207

Huang J, Yi Y, Wang S, Chou J (1993) An analogue-dynamical long-range numerical weather prediction system incorporating historical evolution, Q. J. Roy Meteor Soc. 119 (511), 547.

Kanamitsu M, Ebisuzaki W, Woollen J, Yang S-K, Hnilo JJ, Fiorino M, Potter GL (2002) NCEP-DOE AMIP-II Reanalysis (R-2). Bull Am Meteorol Soc 83:1631

Koster RD, Dirmeyer PA, Zhichang G et al (2004) Regions of strong coupling between soil moisture and precipitation. Science 305(5687):1138

Li J, Yu R, Zhou T (2008) Seasonal variation of the diurnal cycle of rainfall in southern contiguous China. J Clim 21(22):6036

Li X, Zhou W, Li C (2013) Comparison of the annual cycles of moisture supply over Southwest and Southeast China. J Clim 26(24):10139

North GR (1982) Sampling errors in the estimation of empirical orthogonal functions. Mon Weather Rev 110(7):699

Tourre YM, White WB (1995) ENSO signals in global upper-ocean temperature. J Phys Oceanogr 25(6):1317

Venzke S, Latif M, Villwock A (2000) The coupled GCM ECHO-2. Part II: Indian ocean response to ENSO. J Clim 13(8):1371

Wang HJ, Xue F, Zhou GQ (2002) The spring monsoon in South China and its relationship to large-scale circulation features. Adv Atmos Sci 19:651

Wu R, Chen W, Wang G (2014) Relative Contribution of ENSO and East Asian winter monsoon to the South China Sea SST anomalies during ENSO decaying years. J Geophys Res 119(9):5046

Xu WX, Zipser EJ, Liu CT (2009) Rainfall characteristics and convective properties of mei-yu precipitation systems over South China, Taiwan, and the South China Sea. Part I: TRMM observations. Mon Weather Rev 137(12):4261

Xu W, Zipser EJ, Chen YL et al (2012) An orography-associated extreme rainfall event during TiMREX: initiation, storm evolution, and maintenance. Mon Weather Rev 140(8):2555

Yu R, Xu Y, Zhou T et al (2007) Relation between rainfall duration and diurnal variation in the warm season precipitation over central eastern China. Geophys Res Lett 34(13):173

Yuan Y, Zhou W, Chan JCL et al (2008) Impacts of the basin-wide Indian Ocean SSTA on the South China Sea summer monsoon onset. Int J Climatol 28(12):1579

Zhai PM, Zhang XB, Wan H et al (2005) Trends in total precipitation and frequency of daily precipitation extremes over China. J Clim 18:1096

Zhang SX, Feng GL, Zhao JH (2013) "Cumulative effect" of torrential rain in the middle and lower reaches of the Yangtze River. Acta Phys Sin 62:496 (in Chinese)

Zheng Z, Ren H, Huang J (2009) Analogue correction of errors based on seasonal climatic predictable components and numerical experiments. Acta Phys Sin 58(10):7359 (in Chinese)

Zhi R, Lian Y, Feng GL (2007) The influence of different scale systems on precipitation analyzed on the basis of power-law exponent. Acta Phys Sin 56:1837 (in Chinese)

Zhou LT, Wu R (2010) Respective impacts of the East Asian winter monsoon and ENSO on winter rainfall in China. J Geophys Res 115, D02107

Zhou TJ, Yu RC (2005) Atmospheric water vapour transport associated with typical anomalous summer rainfall patterns in China. J Geophys Res 110(D8):211

Zhou T, Wu B, Dong L (2014) Advances in research of ENSO changes and the associated impacts on Asian-Pacific climate. Asia-Pac J Atmos Sci 50(4):405